

# Voltage-controlled liquid-crystal terahertz phase shifter and quarter-wave plate

Cho-Fan Hsieh and Ru-Pin Pan

Department of Electrophysics, National Chiao Tung University,  
Hsinchu, Taiwan 30010

Tsung-Ta Tang, Hung-Lung Chen, and Ci-Ling Pan

Department of Photonics and Institute of Electro-Optical Engineering, National Chiao Tung University, Hsinchu,  
Taiwan 30010

Received November 7, 2005; revised January 2, 2006; accepted January 9, 2006; posted January 23, 2006 (Doc. ID 65847)

Phase shift exceeding  $\pi/2$  at 1 THz is demonstrated by using electrically controlled birefringence in a homeotropically aligned nematic liquid crystal (E7) cell, 570  $\mu\text{m}$  in thickness. The driving voltage required for a phase shift of  $90^\circ$  is 125 V (rms). We demonstrate that the phase shifter works as an electrically switchable quarter-wave plate at 1 THz. The device can also be used as an electrically tuned phase compensator around the quarter-wave point near 1 THz. © 2006 Optical Society of America

OCIS codes: 050.5080, 230.3720, 260.3090, 260.5430, 320.0320.

The past decade has witnessed remarkable progress in terahertz (THz) photonics. THz applications ranging from investigations of ultrafast dynamics in materials to biomedical imaging, environmental sensing, and surveillance were realized.<sup>1–3</sup> For these uses, quasi-optic components such as phase shifters, modulators, attenuators, polarizers, and wave plates are being developed. For example, several groups have demonstrated tunable phase shifters based on optically or electrically controlled carrier concentration in quantum-well structures.<sup>4–6</sup> These quantum-well-based THz phase shifters, however, have limited range of tunability and in general need to be operated at temperatures far below room temperature.<sup>4,5</sup>

The large birefringence of liquid crystals in the visible is well known and has also been employed successfully for phase shifting of microwave and millimeter wave signals previously.<sup>7</sup> In the THz frequency range, we have shown that a nematic liquid crystal (NLC) 4'-n-pentyl-4-cyanobiphenyl (5CB) exhibits relatively large birefringence ( $\sim 0.2$ ) and a small extinction coefficient at frequencies around 1 THz.<sup>8,9</sup> We recently demonstrated the first tunable room-temperature THz phase shifter capable of more than  $360^\circ$  of phase shift at 1 THz.<sup>10,11</sup> The device was based on magnetically controlled birefringence in a sandwiched dual NLC cell. Nonetheless, electrically controlled phase shifters are deemed desirable for many applications. In our previous attempt, a maximum phase shift of  $4.07^\circ$  was achieved at 1.07 THz when the interaction length was 38.6  $\mu\text{m}$  in the homogeneously aligned NLC cell. The driving voltage and corresponding field were 177 V and 589 V/cm, respectively.<sup>12</sup> In this Letter we report electrically tunable phase shifts beyond  $90^\circ$  at 1 THz in a homeotropically aligned NLC cell. The operation of the device as a THz quarter-wave ( $\lambda/4$ ) plate is verified. The experimental results are in good agreement with calculations using the continuum theory of the NLC.

The configuration of this device is shown in Fig. 1. The cell was constructed by sandwiching the E7

(Merck) layer between two fused silica substrates. The thicknesses of the substrate and the E7 layer were  $858 \pm 2$  and  $570 \pm 15$   $\mu\text{m}$ , respectively. Two copper pieces (purity of 99.94%) worked both as spacers and electrodes for the cell. They were parallel to each other and separated by  $11.9 \pm 0.3$  mm. The substrates were coated with *N,N*-dimethyl-*N*-octadecyl-3-aminopropyltrimethoxysilyl chloride (DMOAP) for homeotropic alignment.<sup>13</sup> The alignment was checked by visually examining the unbiased cell. The cell appeared milky and opaque if it was not well aligned. On the other hand, one could see through a well-aligned cell as thick as 0.5 mm. A square-wave ac voltage at 1 kHz was applied to the electrodes. Without the biasing field, the NLC molecules are in the initially stable state and generally perpendicular to the substrates. With positive dielectric anisotropy, the E7 molecules in the bulk of the cell will be reoriented toward the applied electric field once the applied bias is increased beyond the threshold voltage (the Fréedericksz transition<sup>14</sup>),  $V_{\text{th}} = \pi(L/d) \times (k_3/\epsilon_a \epsilon_0)^{1/2}$ , where  $L$  is the distance between two electrodes,  $d$  is the thickness of the NLC layer, and  $k_3$ ,  $\epsilon_a = \epsilon_{\parallel} - \epsilon_{\perp}$ , and  $\epsilon_0$  are the bend elastic constant, dielectric anisotropy, and electric permittivity of free space, respectively. For our device, we calculated that

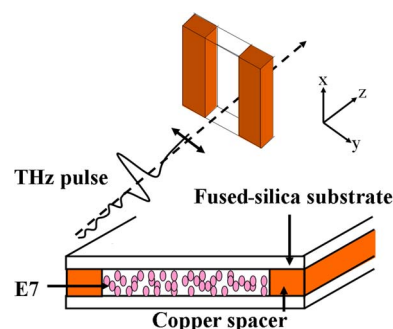


Fig. 1. Schematic drawing of the electrically switched NLC  $\lambda/4$  plate. The THz wave propagation and polarization directions are  $z$  and  $y$ , respectively.

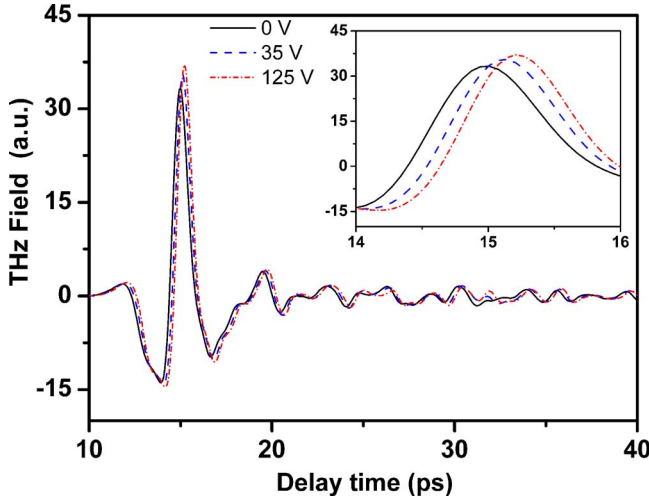


Fig. 2. Temporal waveforms of the THz pulse transmitted through the NLC cell at various driving voltages. The inset is the closeup from 14 to 16 ps.

$V_{\text{th}} = 24.5$  V (rms), with  $L = 11.9$  mm,  $d = 570$   $\mu\text{m}$ ,  $k_3 = 17.1 \times 10^{-12}$  N, and  $\epsilon_a = 13.8$  (from Merck).

The phase shift  $\delta(V)$  experienced by the THz beam transmitted through the cell biased at a voltage  $V$  is given by

$$\delta(V) = \int_0^d \frac{2\pi f}{c} \Delta n_{\text{eff}}(V, z) dz, \quad (1)$$

where  $f$  is the frequency of the THz wave,  $c$  is the speed of light in vacuum, and  $\Delta n_{\text{eff}}(V, z)$  is the change in the effective birefringence for the NLC at a position  $z$  along the propagation direction of the THz beam. The effective birefringence can be written as

$$\Delta n_{\text{eff}} = \left( \frac{\cos^2 \theta}{n_o^2} + \frac{\sin^2 \theta}{n_e^2} \right)^{-1/2} - n_o, \quad (2)$$

where  $n_o$  and  $n_e$  are ordinary and extraordinary indices of refraction of NLC and  $\theta$  is the reorientation-angle of NLC molecules from the original orientation. For  $V > V_{\text{th}}$  the angle  $\theta$  at any point  $z$  in the cell can be computed by using the relation<sup>15</sup>

$$\frac{z}{d} = \frac{V_{\text{th}}}{\pi V} \int_0^\theta \left( \frac{1 + q \sin^2 \theta}{\sin^2 \theta_m - \sin^2 \theta} \right)^{1/2} d\theta, \quad (3)$$

where  $q = (k_1 - k_3)/k_3$  and  $k_1$  ( $= 11.1 \times 10^{-12}$  N for E7) is the splay elastic constant of NLC. The angle  $\theta_m$  is the maximum reorientation angle located at  $z = d/2$ . It is related to  $V/V_{\text{th}}$  by

$$\frac{V}{V_{\text{th}}} = \frac{2}{\pi} \int_0^{\theta_m} \left( \frac{1 + q \sin^2 \theta}{\sin^2 \theta_m - \sin^2 \theta} \right)^{1/2} d\theta. \quad (4)$$

Equations (3) and (4) allow us to calculate the profile of molecular orientation in the cell for a given applied voltage.<sup>15</sup> We further assume that the electric field is uniform, i.e.,  $E = V/d$ .

The device was characterized by a photoconductive-antenna-based THz time-domain spectrometer.<sup>16</sup> Briefly, the pump beam from a femto-

second mode-locked Ti:sapphire laser illuminated the antenna fabricated on low-temperature-grown GaAs to radiate the broadband THz pulse, which was collimated and propagated through the NLC layer between the two electrodes. A pair of parallel wire-grid polarizers (Specac, GS57204 with extinction of  $10^{-3}$ ) was placed with one polarizer before and one after the cell to ensure the polarization state of the THz beam transmitting through the cell. The diameter of the THz beam was  $\sim 8$  mm. The transmitted THz pulse was monitored by the probe beam from the same laser and by using the same kind of antenna. The total duration of the THz scan was 68 ps. The measurements were done at room temperature ( $23 \pm 0.5^\circ\text{C}$ ).

The temporal waveforms of the THz pulse transmitted through the device at several applied voltages are shown in Fig. 2. In the inset of Fig. 2 we show the data from 14 to 16 ps. The transmitted THz pulses exhibit clearly larger delay and higher transmittance at higher applied voltages. This trend is explained by taking into account Fresnel reflections<sup>17</sup> at the two interfaces between the NLC layer<sup>11</sup> ( $n_o = 1.62$ ,  $n_e = 1.79$  at 0.3 THz) and the quartz substrate ( $n = 1.95$  at 0.3 THz). The experimentally measured ratio of transmittance for the  $e$  ray and the  $o$  ray is 1.114, which is almost identical to the theoretically calculated value of 1.113.

Figure 3 shows the phase shift as a function of driving voltage. The curves are theoretical predictions according to Eqs. (1)–(4). They are in good agreement with the experiments. A maximum phase shift of  $93.7^\circ$  was achieved at 1 THz when the cell was driven at 125 V (rms) or 105 V/cm. The theoretically predicted phase shift was  $90.8^\circ$ . The threshold voltage and the corresponding field were found to be 27 V and 22.6 V/cm, respectively, also in excellent agreement with the theoretically predicted value, 24.5 V (rms). For a given voltage, the measured phase shift varied linearly with frequency, with a slope of  $\sim 89.6$  deg/THz at 125 V (rms).

To confirm that the present device can be used as a  $\lambda/4$  plate, we also recorded the transmittance through the device as it was rotated with angle  $\phi$

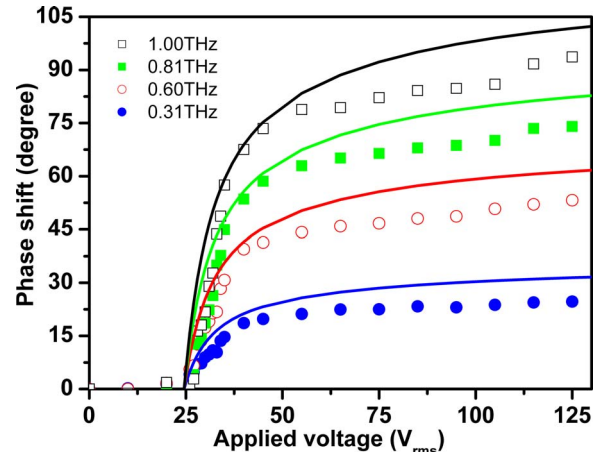


Fig. 3. Phase shift as a function of driving voltage for four frequencies. The solid curves are from the theoretical prediction.

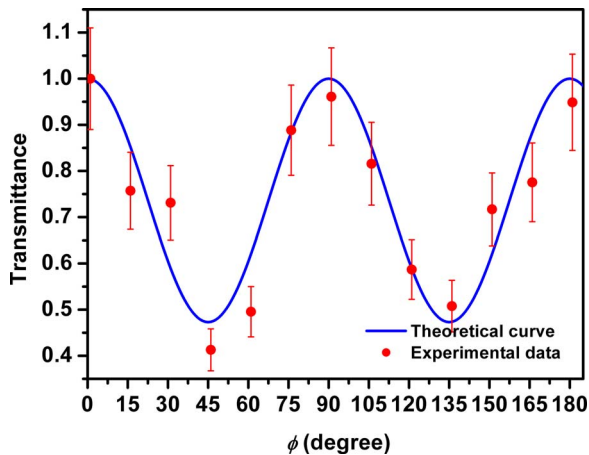


Fig. 4. Transmittance of the device as it was rotated about the THz beam propagation axis. The solid curve is the transmittance for an ideal  $\lambda/4$  plate.

about the axis of propagation (Fig. 4). The results (filled circles) clearly show the squared sinusoidal law dependence for the transmittance and the correct period for a  $\lambda/4$  plate. The transmittance of an ideal  $\lambda/4$  plate,  $1 - (1/2)\sin^2(2\phi)$ , is also plotted as the solid curve, which fits the experimental data without any adjustable parameter. The error bar is due to Ti: sapphire laser power fluctuation and possibly scattering losses by the THz beam propagating through the NLC layer. The latter mechanism is currently under investigation. The dynamics of the cell is determined by its viscosity and geometry of the cell. For our device, the  $1/e$  switching-off time<sup>15</sup> is  $\tau_{\text{off}} = \gamma L^2 / V_{\text{th}}^2 \epsilon_a \epsilon_0$ , where  $\gamma$  is the rotational viscosity. With a typical value of 0.1 Pa s for  $\gamma$ ,<sup>18</sup> we estimate that  $\tau_{\text{off}} \sim 170$  s. Experimentally, we determined the switch-off time by turning off the driving voltage while monitoring the change in the value of the transmitted THz waveform at a fixed delay of the gating optical pulse and obtained  $\tau_{\text{off}} \sim 190$  s.

Although the electrically controlled NLC THz phase shifter has many advantages, we should point out that it is difficult to tune the desired phase shift accurately from 27 to 35 V, near the threshold. From this perspective, the continuously tunable magnetically controlled THz phase shifter in our previous work is superior.<sup>11</sup>

Alternatively, one can design a homogeneously aligned cell with NLCs of negative dielectric anisotropy. In principle, E7, with positive dielectric anisotropy, can also be used in a homogeneously aligned NLC cell with transparent top and bottom electrodes.

In summary, a maximum phase shift of  $93.7^\circ$  at 1 THz is realized by using electrically controlled birefringence in a homeotropically aligned NLC cell. The driving voltage and corresponding field required for a phase shift of  $90^\circ$  are 125 V (rms) and 105 V/cm, respectively. The operation of the phase shifter as a  $\lambda/4$  plate at 1 THz was also demonstrated. In addition, the device can be used as an all-electric precision-tuned phase compensator around the  $\lambda/4$  point.

This work was supported by the National Science Council of the Republic of China under grants NSC 93-2752-E-009-007-PAE and 93-2251-E-009-065. R.-P. Pan's e-mail address is rpchao@mail.nctu.edu.tw; C.-L. Pan's e-mail address is clpan@faculty.nctu.edu.tw

## References

1. D. Grischkowsky, S. R. Keiding, M. V. Exter, and C. Fattinger, *J. Opt. Soc. Am. B* **7**, 2006 (1990).
2. B. Ferguson and X.-C. Zhang, *Nat. Mater.* **1**, 26 (2002).
3. D. Mittleman, *Sensing with THz Radiation* (Springer, 2002).
4. I. H. Libon, S. Baumgärtner, M. Hempel, N. E. Hecker, J. Feldmann, M. Koch, and P. Dawson, *Appl. Phys. Lett.* **76**, 2821 (2000).
5. R. Kersting, G. Strasser, and K. Unterrainer, *Electron. Lett.* **36**, 1156 (2000).
6. T. Kleine-Ostmann, P. Dawson, K. Pierz, G. Hein, and M. Koch, *Appl. Phys. Lett.* **84**, 3555 (2004).
7. K. C. Lim, J. D. Margerum, and A. M. Lackner, *Appl. Phys. Lett.* **62**, 1065 (1993).
8. T.-R. Tsai, C.-Y. Chen, C.-L. Pan, R.-P. Pan, and X.-C. Zhang, *Appl. Opt.* **42**, 2372 (2003).
9. R.-P. Pan, T.-R. Tsai, C.-Y. Chen, C.-H. Wang, and C.-L. Pan, *Mol. Cryst. Liq. Cryst.* **409**, 137 (2004).
10. C.-Y. Chen, T.-R. Tsai, C.-L. Pan, and R.-P. Pan, *Appl. Phys. Lett.* **83**, 4497 (2003).
11. C.-Y. Chen, C.-F. Hsieh, Y.-F. Lin, R.-P. Pan, and C.-L. Pan, *Opt. Express* **12**, 2630 (2004).
12. T.-R. Tsai, C.-Y. Chen, R.-P. Pan, C.-L. Pan, and X.-C. Zhang, *IEEE Microw. Wirel. Compon. Lett.* **14**, 77 (2004).
13. F. J. Kahn, *Appl. Phys. Lett.* **22**, 386 (1973).
14. P. G. de Gennes and J. Prost, *The Physics of Liquid Crystals*, 2nd ed. (Oxford, 1983).
15. S. Chandrasekhar, *Liquid Crystal*, 2nd ed. (Cambridge, 1992).
16. C.-L. Pan, C.-F. Hsieh, R.-P. Pan, M. Tanaka, F. Miyamaru, M. Tani, and M. Hangyo, *Opt. Express* **13**, 3921 (2005).
17. E. Hecht, *Optics*, 3rd ed. (Addison Wesley-Longman, 1998).
18. K. Skarp, S. T. Lagerwall, and B. Stebler, *Mol. Cryst. Liq. Cryst.* **60**, 215 (1980).